UNIVERSITY OF
BATH

Citation for published version:
Klein, A, Bruderer, M, Clark, SR & Jaksch, D 2007, 'Dynamics, dephasing and clustering of impurity atoms in Bose-Einstein condensates', *New Journal of Physics*, vol. 9, 202, pp. 1 - 22. https://doi.org/10.1088/1367-2630/9/11/411

DOI:
10.1088/1367-2630/9/11/411

Publication date:
2007

Document Version
Early version, also known as pre-print

Link to publication

Publisher Rights
CC BY

This is a submitted version of an article published by IOP Publishing in Klein, A, Bruderer, M, Clark, SR & Jaksch, D 2007, 'Dynamics, dephasing and clustering of impurity atoms in Bose-Einstein condensates' New Journal of Physics, vol 9, 202, pp. 1 - 22., 10.1088/1367-2630/9/11/411

University of Bath

Dynamics, dephasing and clustering of impurity atoms in Bose-Einstein condensates

Alexander Klein[1,2]**, Martin Bruderer**[1]**, Stephen R. Clark**[1,3]**, and Dieter Jaksch**[1,2]

[1]Clarendon Laboratory, University of Oxford, Parks Road, Oxford OX1 3PU, United Kingdom

[2] Keble College, Parks Road, Oxford OX1 3PG, United Kingdom

[3] Trinity College, Broad Street, Oxford OX1 3BH, United Kingdom

Abstract.
We investigate the influence of a Bose-Einstein condensate (BEC) on the properties of immersed impurity atoms, which are trapped in an optical lattice. Assuming a weak coupling of the impurity atoms to the BEC, we derive a quantum master equation for the lattice system. In the special case of fixed impurities with two internal states the atoms represent a quantum register and the quantum master equation reproduces the exact evolution of the qubits. We characterise the qubit dephasing which is caused by the interspecies coupling and show that the effect of sub- and superdecoherence is observable for realistic experimental parameters. Furthermore, the BEC phonons mediate an attractive interaction between the impurities, which has an important impact on their spatial distribution. If the lattice atoms are allowed to move, there occurs a sharp transition with the impurities aggregating in a macroscopic cluster at experimentally achievable temperatures. We also investigate the impact of the BEC on the transport properties of the impurity atoms and show that a crossover from coherent to diffusive behaviour occurs with increasing interaction strength.

1. Introduction

Ultracold atoms in optical lattices have attracted considerable interest during the last few years. Theoretical investigations showed that ultracold atoms in optical lattices can be used for mimicking a wide range of models encountered in condensed matter physics [1]. These models include the Hubbard Hamiltonian [2, 3], spin-spin interactions [4, 5], high-temperature superconductivity [6, 7], effective magnetic fields [8–13], even with non-abelian gauge potentials [14, 15], and the fractional quantum Hall effect [13, 16], to name but a few. Experimental efforts have led to an unprecedented control over the properties of optical lattice systems [17], including such milestones as the Mott insulator to superfluid transition [18,19], investigations of Bose-Fermi [20,21] as well as Bose-Bose mixtures [22], vortex pinning [23], the creation of repulsively bound atom pairs [24], and cold controlled collisions between atoms in optical lattices [25, 26]. Especially for the latter experiments the absence of lattice phonons and thus the suppression of decoherence mechanisms was crucial. However, when mimicking the behaviour of electrons in crystals this lack of phonons might lead to an oversimplification of the underlying model and it is desirable to introduce phonons in a controlled manner into the optical lattice system.

One way of achieving this goal is to immerse the optical lattice system into a Bose-Einstein condensate (BEC). Experiments where both atom species are trapped by the optical lattice are common and decoherence effects in such systems have already been observed [20, 21]. Furthermore, these Bose-Fermi mixtures promise rich phase diagrams including charge and spin density wave phases [27, 28], pairing of fermions with bosons [29] and a supersolid phase [30]. We, however, focus on the case where only one species is trapped by the optical lattice. This can be achieved by a suitable choice of the laser wavelengths and atomic species such that the BEC is not affected by the optical lattice [31]. The lattice atoms interact with the condensate via density-density interaction, which can be described by Bogoliubov phonons coupling to the impurities. Earlier studies on such systems have shown that this coupling can be exploited to cool the lattice atoms to extremely low temperatures [32, 33], which are otherwise very difficult to achieve. In Ref. [34], the present authors have derived a model in which lattice atoms dressed by a coherent state of Bogoliubov phonons constitute polarons [35]. The model exhibits an attractive interaction potential between the lattice atoms [36, 37] and allows a generalised master equation to be deduced which shows that the system exhibits a crossover from coherent to diffusive dynamics.

Instead, in this work we concentrate on describing the lattice atoms by a quantum master equation (QME), which is derived in Sec. 3. We show in Sec. 4 that for the case of fixed impurities the system can be solved exactly and after tracing out the BEC degrees of freedom the QME reproduces this exact solution. Due to the coupling to the phonons the lattice atoms experience dephasing, which can be used to demonstrate the effects of sub- and superdecoherence [38] and to probe spatial properties of the BEC analogous to Ref. [39]. We also investigate the severe effect this decoherence has if the atoms in the lattice are used as a quantum register. In Sec. 5 we show that the attractive interaction mediated between the lattice atoms leads to the formation of atom clusters, which should be observable for typical experimental parameter regimes. This effect is reminiscent of the clustering of ad-atoms on crystal surfaces [40]. The influence of the phonon coupling on the transport properties of the lattice atoms is investigated in Sec. 6. We show that the crossover from coherent to diffusive transport, which was observed in Ref. [34], can also be described by the QME. In contrast to the
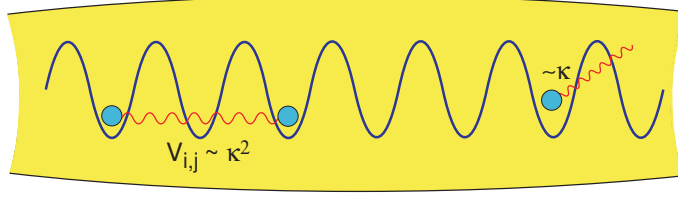
Figure 1. An ultracold quantum gas trapped in an optical lattice is immersed in a much larger BEC. The impurities interact with the BEC via the coupling constant κ and can excite Bogoliubov phonons (right). These lead to dephasing effects. By exchanging phonons an off-site interaction $V_{i,j}$ is mediated between the lattice atoms (left).

treatment in Ref. [34], the QME in addition gives access to the off-diagonal elements of the density operator. We also show the limitations of the QME by applying it to a tilted lattice system and comparing the results to a near-exact numerical solution for the time evolution.

2. Model

The system under consideration is composed of a BEC and an ultracold gas of impurity atoms trapped in an optical lattice giving a setup like that shown in Fig. 1. The impurities can be either bosonic or fermionic atoms. For most of the results derived in this work the statistics of the lattice atoms is unimportant, but for concreteness we will assume bosonic impurities in the following. The dynamics of the whole system is governed by the Hamiltonian $\hat{H} = \hat{H}_{\mathrm{L}} + \hat{H}_{\mathrm{B}} + \hat{H}_{\mathrm{I}}$, where

$$\hat{H}_{\mathrm{B}} = \int \mathrm{d}\mathbf{r}\, \hat{\phi}^{\dagger}(\mathbf{r}) \left[-\frac{\hbar^2 \nabla^2}{2m_b} + V_{\mathrm{ext}}(\mathbf{r}) + \frac{g}{2}\hat{\phi}^{\dagger}(\mathbf{r})\hat{\phi}(\mathbf{r}) \right] \hat{\phi}(\mathbf{r}) \tag{1}$$

describes the BEC, with $\hat{\phi}^{\dagger}$ the condensate field operator, m_b the mass of the BEC atoms, $V_{\mathrm{ext}}(\mathbf{r})$ an external potential confining the BEC, and $g > 0$ the coupling constant between the BEC atoms. Here, we have assumed that the optical lattice potential does not affect the BEC atoms, which can be achieved by choosing the laser wavelengths and atom species accordingly [31]. The atoms in the optical lattice, which are distinguishable from the atoms in the BEC, are described by the Hamiltonian $\hat{H}_{\mathrm{L}}$, whereas the interaction between the two sub-systems is given by

$$\hat{H}_{\mathrm{I}} = \kappa \int \mathrm{d}\mathbf{r}\, \hat{\chi}^{\dagger}(\mathbf{r})\hat{\chi}(\mathbf{r})\hat{\phi}^{\dagger}(\mathbf{r})\hat{\phi}(\mathbf{r})\,. \tag{2}$$

Here, $\hat{\chi}^{\dagger}$ is the field operator of the lattice atoms, and κ is the density-density coupling constant between the BEC and the impurities. It was shown in Ref. [34] that in the tight-binding limit and under the condition $|\kappa|/gn_0\xi^D \ll 1$ (where D is the dimensionality of the system, n_0 the density of the BEC in the trap centre, and $\xi = \hbar/\sqrt{m_b gn_0}$ the healing length) the total Hamiltonian reduces to a Hubbard-Holstein model, given by

$$\hat{H}_{\mathrm{L}} = -J \sum_{\langle i,j \rangle} \hat{a}_j^{\dagger}\hat{a}_i + \frac{U}{2}\sum_i \hat{n}_i(\hat{n}_i - 1) + \mu \sum_i \hat{n}_i\,, \tag{3}$$

$$\hat{H}_{\mathrm{I}} = \sideset{}{'}\sum_{\nu}\sum_{j} \hbar\omega_\nu \left[M_{j,\nu}\hat{b}_\nu + M_{j,\nu}^*\hat{b}_\nu^\dagger \right] \hat{n}_j \,, \tag{4}$$

$$\hat{H}_{\mathrm{BEC}} = \sideset{}{'}\sum_{\nu} \hbar\omega_\nu \hat{b}_\nu^\dagger \hat{b}_\nu \,. \tag{5}$$

Here, the prime at the sum indicates that zero energy modes have been excluded, $\hat{b}_\nu^\dagger$ creates a Bogolibov phonon in mode ν with energy $\hbar\omega_\nu$, $\hat{a}_j^\dagger$ creates a lattice atom in site j, $\hat{n}_j = \hat{a}_j^\dagger \hat{a}_j$ is the number operator on site j, J describes the hopping of the impurities, U is their on-site interaction, and the coupling between the phonons and the lattice atoms is given by

$$F_{j,\nu} = \hbar\omega_\nu M_{j,\nu} = \kappa \int \mathrm{d}\mathbf{r}\, \phi_0(\mathbf{r}) \left[u_\nu(\mathbf{r}) - v_\nu(\mathbf{r}) \right] |\eta_j(\mathbf{r})|^2 \,. \tag{6}$$

In this equation, η_j is a Wannier function describing an atom in lattice site j, ϕ_0 is the solution of the Gross-Pitaevskii equation and u_ν and v_ν solve the Bogoliubov-de Gennes equations, see also Ref. [41].

For the case of a homogenous condensate, which we consider in the remainder of the paper, the expressions for the atom-phonon coupling is given by

$$F_{j,\mathbf{q}} = \kappa \sqrt{\frac{n_0 \varepsilon_\mathbf{q}}{\hbar\omega_\mathbf{q}}}\, f_j(\mathbf{q}) \,, \tag{7}$$

where $\mathbf{q}$ is the phonon quasi-momentum, $\varepsilon_\mathbf{q} = (\hbar\mathbf{q})^2/2m_b$ the free particle energy, $\hbar\omega_\mathbf{q} = \sqrt{\varepsilon_\mathbf{q}(\varepsilon_\mathbf{q} + 2gn_0)}$ the Bogoliubov dispersion relation and $f_j(\mathbf{q}) = \Omega^{-1/2}\int \mathrm{d}\mathbf{r}|\eta_j(\mathbf{r})|^2 \exp(\mathrm{i}\mathbf{q}\cdot\mathbf{r})$, with Ω the quantisation volume. The latter integral can in general not be solved analytically. However, for sufficiently deep lattices [42], the Wannier functions can be approximated by Gaussians, yielding

$$f_j(\mathbf{q}) = \frac{\mathrm{e}^{\mathrm{i}\mathbf{q}\cdot\mathbf{r}_j}}{\sqrt{\Omega}} \exp\left(-\frac{1}{4}\sum_{l=1}^{D} q_l^2 x_0^2 \right) \,, \tag{8}$$

with $x_0 = \sqrt{\hbar/m_b\omega_\mathrm{t}}$, where ω_t is the trapping frequency of a harmonic trap approximating the lattice potential at a given lattice site.

An experimental realisation of this setup is achievable with present techniques as follows. The creation of Rb condensates with 10^6 atoms has been demonstrated leading to the desired BEC densities of about $10^{20}/\mathrm{m}^3$ in three dimensions, see for instance [43]. By choosing a sufficiently flat trapping potential of a few Hz the BEC can be assumed to be homogenous to a good approximation in the centre of the trap, extending over a few micrometers. Furthermore, in references [20, 21] a mixture of Rb and K atoms has been created and trapped in a three-dimensional optical lattice, where several tens of thousands of lattice sites have been occupied. The filling for the K atoms ranged between 0 and 1 atoms per lattice site, whereas the filling of the Rb atoms could exceed 5 atoms per site in the centre of the trap. Although in these experiments both atom species were trapped by the optical lattice, techniques to trap only one of the two species, for example K, have been studied extensively in reference [31]. Applying these techniques leaves the Rb atoms virtually unaffected and enables the creation of a nearly homogenous BEC.

3. The quantum master equation

In order to investigate the behaviour of the impurity atoms we derive a Quantum Master Equation (QME) for the lattice system by tracing out the surrounding BEC. The details are given in Appendix A. Here we note that the main condition of deriving the QME is that the sound velocity of the condensate, $c \sim \sqrt{gn_0/m_b}$, is larger than the typical hopping speed of the atoms, i.e., $c \gg Ja/\hbar$, where $a = \lambda/2$ is the distance between two lattice sites. With this assumption we get

$$i\hbar\partial_t\hat{\varrho}_L(t) = \left[\hat{H}_g(t), \hat{\varrho}_L(t)\right] - \frac{i}{\hbar}\sum_{\mathbf{q}}{}' \sum_{l,l'} \frac{\sin(\omega_\mathbf{q}t)}{\omega_\mathbf{q}}(\hat{n}_l\hat{n}_{l'}\hat{\varrho}_L(t) + \hat{\varrho}_L(t)\hat{n}_l\hat{n}_{l'} - 2\hat{n}_{l'}\hat{\varrho}_L(t)\hat{n}_l)$$
$$\times \left(F_{\mathbf{q},l}F^*_{\mathbf{q},l'} + N_\mathbf{q}(T)(F_{\mathbf{q},l}F^*_{\mathbf{q},l'} + F^*_{\mathbf{q},l}F_{\mathbf{q},l'})\right). \qquad (9)$$

Here, $N_\mathbf{q}(T) = 1/(\exp(\hbar\omega_\mathbf{q}/k_BT) - 1)$ is the number of thermal phonons at temperature T, and $\hat{\varrho}_L(t) = \mathrm{Tr}_B\hat{\varrho}(t)$, where Tr_B denotes the trace over the condensate. Furthermore, the Hamiltonian

$$\hat{H}_g(t) = \hat{H}_L - \sum_{\mathbf{q}}{}' \sum_{l,l'} \frac{1 - \cos(\omega_\mathbf{q}t)}{2\hbar\omega_\mathbf{q}}(F_{\mathbf{q},l}F^*_{\mathbf{q},l'} + F^*_{\mathbf{q},l}F_{\mathbf{q},l'})\hat{n}_l(t)\hat{n}_{l'}(t) \qquad (10)$$

describes the coherent evolution of the lattice atoms, most notably an off-site interaction which is mediated by the phonons of the BEC. The interaction term includes a transient behaviour described by the cosine functions, which accounts for suddenly turning on the interaction between lattice atoms and BEC. The sum over all these cosine functions vanishes in the limit $t \to \infty$.

The Born approximation used in deriving the QME is valid if the perturbation caused by the BEC is small compared to the typical energy scales given by the lattice system. If only the hopping term is important for the lattice atoms, this energy scale is determined by J. The energy scale of the perturbation is given by the so-called polaron energy $E_p = \sum_{\mathbf{q}}{}'(F_{\mathbf{q},l}F^*_{\mathbf{q},l} + F^*_{\mathbf{q},l}F_{\mathbf{q},l})/2\hbar\omega_\mathbf{q} \sim \kappa^2/g\xi^D$, which leads to the condition $J \gg E_p$. This parameter regime is complementary to the one considered in Ref. [34], where the opposite limit was investigated. As we will show in the following section, the condition $J \gg E_p$ is not required for the case of $J = 0$, where an analytical solution of the dynamics of the whole system can be derived. After tracing out the BEC degrees of freedom this solution agrees with the one given by the QME.

4. Fixed impurities and the Quantum Register

For very deep optical lattices the hopping constant J is essentially zero and the impurities cannot leave their site. If there is a maximum of one atom in each lattice site, the setup can be used as a quantum register [44]. The lattice atoms represent qubits on which single qubit rotations can be implemented via external laser pulses. For the manipulation of the atoms single site addressability is necessary, which may be achieved by using infrared lattices [45], by leaving empty sites between the atoms [46, 47], by exploiting the properties of marker atoms [48], or by additional external fields [49, 50]. An entangling two-qubit gate can be implemented by using the interaction which is mediated by the condensate [37]. For this it is necessary to turn the interaction on and off, which can be done by using different internal states of the lattice atoms, some of which couple to the BEC, and others that do not couple. However, due to the coupling to the BEC the qubits also experience dephasing, which will be investigated in this section.

4.1. Analytical solution of the time evolution

We first calculate the time evolution of the atoms subject to the BEC coupling. For easier notation we focus on the case where the lattice atoms have only one internal state and we assume that there is a maximum of one atom per lattice site. In the regime were our model introduced in section 2 is valid, i.e. $|\kappa|/gn_0\xi^D \ll 1$, and for $J = 0$, the Hamiltonian of the whole system simplifies to $\hat{H}_0 = \hat{H}_{\text{BEC}} + \hat{H}_{\text{I}}$, where $\hat{H}_{\text{I}}$ is given in Eq. (4) and $\hat{H}_{\text{BEC}}$ in Eq. (5). The time evolution $\hat{U}(t) = \exp(-i\hat{H}_0 t/\hbar)$ of this Hamiltonian is solved analytically. We first note that $\hat{U}(t) = \prod_{\mathbf{q}}' \hat{U}_{\mathbf{q}}(t)$ with

$$\hat{U}_{\mathbf{q}}(t) = \exp\left[-i\left(\hbar\omega_{\mathbf{q}}\hat{b}_{\mathbf{q}}^{\dagger}\hat{b}_{\mathbf{q}} + \sum_l \hat{n}_l(F_{l,\mathbf{q}}\hat{b}_{\mathbf{q}} + F_{l,\mathbf{q}}^*\hat{b}_{\mathbf{q}}^{\dagger})\right)\frac{t}{\hbar}\right]. \tag{11}$$

This operator can be decomposed using the methods described in Ref. [51], yielding

$$\hat{U}_{\mathbf{q}}(t) = \exp\left[-i\omega_{\mathbf{q}}\hat{b}_{\mathbf{q}}^{\dagger}\hat{b}_{\mathbf{q}}t\right]\exp\left[\sum_l \hat{n}_l(\tilde{F}_{l,\mathbf{q}}\hat{b}_{\mathbf{q}} - \tilde{F}_{l,\mathbf{q}}^*\hat{b}_{\mathbf{q}}^{\dagger})\right]$$

$$\times \exp\left[\frac{i(\omega_{\mathbf{q}}t - \sin(\omega_{\mathbf{q}}t))}{2\hbar^2\omega_{\mathbf{q}}^2}\sum_{l,l'}\hat{n}_l\hat{n}_{l'}(F_{l,\mathbf{q}}F_{l',\mathbf{q}}^* + F_{l,\mathbf{q}}^*F_{l',\mathbf{q}})\right]. \tag{12}$$

Here, we have defined $\tilde{F}_{l,\mathbf{q}} = F_{l,\mathbf{q}}\left[-i\sin(\omega_{\mathbf{q}}t) - (1 - \cos(\omega_{\mathbf{q}}t))\right]/\hbar\omega_{\mathbf{q}}$. The last term in Eq. (12) describes the off-site interaction between two atoms confined in lattice sites l and l', which is mediated by a phonon with quasi-momentum $\mathbf{q}$. The total interaction potential is derived by adding all phonon contributions together. For $t \to \infty$, the oscillations caused by the sine function cancel each other and the off-site interaction potential is given by†

$$V_{l,l'} = \sum_{\mathbf{q}}' \frac{F_{l,\mathbf{q}}F_{l',\mathbf{q}}^* + F_{l,\mathbf{q}}^*F_{l',\mathbf{q}}}{2\hbar\omega_{\mathbf{q}}}. \tag{13}$$

This interaction potential was already found earlier [34,37], however, the exact solution in addition reveals the transient behaviour after suddenly turning on the interaction, which is described by the sine functions.

The coupling to the BEC leads to dephasing of the lattice atoms as gets apparent after tracing out the condensate degrees of freedom. There are in essence two different types of dephasing. One can be observed when a lattice atom is driven into a superposition of two different states which couple differently to the condensate. This situation has been discussed in reference [39]. The other type of dephasing is given when comparing the phase of two atoms in different lattice sites. We illustrate this effect of dephasing by calculating the correlation function $\langle\hat{a}_\gamma^\dagger\hat{a}_\beta\rangle = \text{Tr}\left[\hat{a}_\gamma^\dagger\hat{a}_\beta\hat{\varrho}(t)\right] = \text{Tr}\left[\hat{U}^\dagger(t)\hat{a}_\gamma^\dagger\hat{U}(t)\hat{U}^\dagger(t)\hat{a}_\beta\hat{U}(t)\hat{\varrho}(0)\right]$. A combination of the two dephasing effects is discussed in section 4.2.

If we choose the same initial conditions as in Appendix A, namely $\hat{\varrho}(0) = \hat{\varrho}_{\text{L}}(0) \otimes \hat{\varrho}_{\text{B}}(0)$ and $\hat{\varrho}_{\text{B}}(0)$ describes a thermal state of the BEC, we get

$$\langle\hat{a}_\gamma^\dagger\hat{a}_\beta\rangle = \text{Tr}_{\text{L}}\left[\exp\left(\frac{i}{\hbar}\int_0^t \hat{H}_g(s)\,\mathrm{d}s\right)\tilde{a}_\gamma^\dagger(0)\tilde{a}_\beta(0)\exp\left(-\frac{i}{\hbar}\int_0^t \hat{H}_g(s)\,\mathrm{d}s\right)\tilde{\varrho}_L(0)\right] \times$$

---

† For later convenience, we define this $V_{l,l'}$ in such a way that the interaction term in the Hamiltonian is given by $-\sum_{l,l'} V_{l,l'}\hat{n}_l\hat{n}_{l'}$.

$$\exp\left(-\sideset{}{'}\sum_{\mathbf{q}} \frac{1}{\hbar^2\omega_{\mathbf{q}}^2} |F_{\beta,\mathbf{q}} - F_{\gamma,\mathbf{q}}|^2 (1 - \cos(\omega_{\mathbf{q}}t))(2N_{\mathbf{q}}(T) + 1)\right). \tag{14}$$

Here, $\mathrm{Tr_L}$ denotes the trace over the lattice system, $\hat{H}_g$ was introduced in Eq. (10), and we made use of the identity $\mathrm{Tr_B}\left[\exp(\alpha_{\mathbf{q}}\hat{b}_{\mathbf{q}}^{\dagger} - \alpha_{\mathbf{q}}^*\hat{b}_{\mathbf{q}})\hat{\varrho}_B\right] = \exp[-|\alpha_{\mathbf{q}}|^2(2N_{\mathbf{q}}(T) + 1)/2]$ for thermally distributed $\hat{\varrho}_B$ and some complex number $\alpha_{\mathbf{q}}$ [52]. The first part of Eq. (14) describes the correlations between lattice sites γ and β which are induced by the dynamics of the lattice atoms. In our case, their time evolution only contributes a phase term. The second part describes the dephasing which is caused by the coupling to the BEC atoms. Let us denote the dephasing term by Γ. In the thermodynamic limit of the Bogoliubov modes we can replace the sum by an integral and get

$$\Gamma \geq \exp\left(-\sideset{}{'}\sum_{\mathbf{q}} \frac{8d_{\mathbf{q}}}{(\hbar\omega_{\mathbf{q}})^2}(2N_{\mathbf{q}}(T) + 1)\right)$$

$$\approx \exp\left(-\int \mathrm{d}^D\mathbf{k} \frac{8\kappa^2}{(2\pi)^D g^2 n_0 \xi^D} \frac{\exp(-\mathbf{k}^2 x_0^2/2\xi^2)}{k\sqrt{k^2 + 2}^3}(2N_{\mathbf{k}}(T) + 1)\right) =: \Gamma_{\min}, \tag{15}$$

where $d_{\mathbf{q}} = \kappa^2 n_0 \varepsilon_{\mathbf{q}} \exp(-\mathbf{q}^2 x_0^2/2)/\Omega\hbar\omega_{\mathbf{q}}$, $F_{\mathbf{q},j} = \sqrt{d_{\mathbf{q}}}\exp(i\mathbf{q}\mathbf{r}_j)$, and D is the number of spatial dimensions. For zero temperature, $D = 3$, and $\xi \gg x_0$ the integral can be approximated by neglecting the exponential function which gives $\Gamma(T = 0) \geq \exp(-4\kappa^2/\sqrt{2}\pi^2 g^2 n_0\xi^3)$, whereas for sufficiently high finite temperature $k_B T \gg gn_0$ we find $\Gamma \geq \exp(-\kappa^2 k_B T/\sqrt{2}\pi g^3 n_0^2\xi^3)$. In both cases the factor Γ describing the dephasing fulfils $\Gamma > \varsigma > 0$ for a suitable real number ς. This is independent of time or of the distance between the two atoms, which is different from the one-dimensional case, where numerical calculations show that Γ decays to 0 in the thermodynamic limit for $t \to \infty$ as well as for $|r_\gamma - r_\beta| \to \infty$, indicating that no correlations survive.

Interestingly, the solution of the QME introduced in Sec. 3 gives the same correlation functions, which also holds for the time evolution of the operators $\hat{a}_j$ after tracing out the condensate. This is due to the fact that the interaction commutes with the lattice Hamiltonian for $J = 0$ and that the BEC is initially in a Gaussian, namely a thermal, state [53]. Hence, for the case $J = 0$ the QME describes the lattice atoms exactly after the trace over the BEC is taken. For $J \neq 0$ the interaction Hamiltonian and the one describing the lattice atoms do no longer commute, and the QME is only valid for a large hopping with $J \gg E_p$.

## 4.2. Sub- and superdecoherence and probing the BEC

It has been predicted in Ref. [38] that decoherence effects caused by a qubit-bath coupling can be enhanced (superdecoherence) or suppressed (subdecoherence) for certain cases.‡ Here we show that these effects are indeed observable in a BEC for realistic experimental parameters. The effect can moreover be used in order to probe such BEC properties as the temperature with different sensitivity, similar to the method introduced in Ref. [39].

Let us assume that the atoms have two internal states $|0\rangle$ and $|1\rangle$ which couple to the BEC with different coupling constants $\kappa_0 = 0$, $\kappa_1 = \kappa$. This case can be

---

‡ In our case it would be more appropriate to speak of sub- and superdephasing. We will however stick to the conventions introduced in Ref. [38].
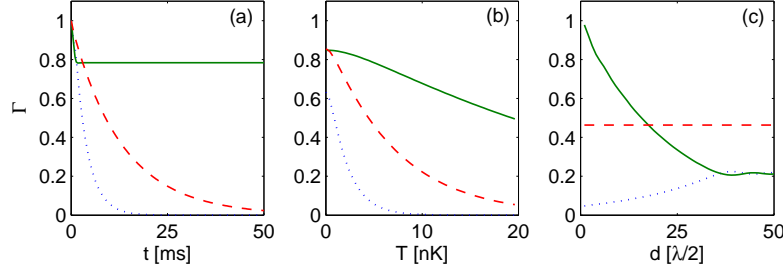
Figure 2. The different behaviour of the dephasing functions Γ_- (solid line), Γ_0 (dashed line) and Γ_+ (dotted line) versus (a) time, (b) temperature, and (c) distance d of the lattice atoms. Two ^{133}Cs atoms were assumed in an optical lattice with wavelength $\lambda = 790$nm and a depth of $V_0 = 40E_R$, where $E_R = (2\pi\hbar)^2/2m_l\lambda^2$. The one-dimensional BEC consists of ^{87}Rb atoms with a linear number density of $5\times10^6/$m. The couplings are given by $g = 4.5\times10^{-2}E_R\lambda$ and $\kappa = 3.5\times10^{-2}E_R\lambda$. In (a), a temperature of $T = 5$nK and a distance of $d = 5\lambda/2$ were chosen, in (b) the same distance and a time of $t = 10$ms, in (c) $T = 5$nK and $t = 10$ms. For recent experiments of RbCs-mixtures, see Refs. [55, 56].

easily generalised to a non-zero κ_0. The different coupling strengths can for example be realised in a ^{40}K$-^{87}$Rb mixture. The positions of the Feshbach resonances for the scattering with the rubidium atoms depends on the fine structure levels $|F, m_F\rangle$ of the potassium atoms [54]. By choosing the external magnetic field close to one Feshbach resonance considerable differences between the scattering lengths and hence the coupling constants for different internal states can be achieved, and it is even possible to tune one scattering length to zero.

Initially, the total state of the two atoms is described by the density matrix $\hat{\varrho}_{\mathbf{2}}(0) = \sum_{ijkl=0,1} \varrho_{ijkl}(0)|ij\rangle\langle kl|$. After evolving for a certain time t and tracing out the BEC the density matrix changes to $\hat{\varrho}_{\mathbf{2}}(t) = \hat{U}_{\text{coh}} \sum_{ijkl=0,1} \overline{\varrho}_{ijkl}(t)|ij\rangle\langle kl|\hat{U}^{\dagger}_{\text{coh}}$, where $\hat{U}_{\text{coh}}$ describes the coherent evolution of the atoms induced by the off-site interaction term, which for our case only changes the phase of the matrix elements, but not their absolute value. The elements $\overline{\varrho}_{ijkl}(t)$ are given by $\overline{\varrho}_{ijkl}(t) = \varrho_{ijkl}(0)$ if $i = k$ and $j = l$, $\overline{\varrho}_{ijkl}(t) = \Gamma_0 \varrho_{ijkl}(0)$ if $i + j + k + l$ is an odd number, $\overline{\varrho}_{ijkl}(t) = \Gamma_- \varrho_{ijkl}(0)$ for ϱ_{0110} and ϱ_{1001} and $\overline{\varrho}_{ijkl}(t) = \Gamma_+ \varrho_{ijkl}(0)$ for ϱ_{1100} and ϱ_{0011}. The functions $\Gamma_{+,0,-}$ are calculated analogously to the dephasing term Γ in Sec. 4.1 and are given by

$$\Gamma_0 = \exp\left(-\sideset{}{'}\sum_{\mathbf{q}} d_{\mathbf{q}} \frac{1 - \cos(\omega_{\mathbf{q}}t)}{(\hbar^2\omega_{\mathbf{q}})^2}(2N_{\mathbf{q}}(T) + 1)\right), \tag{16}$$

$$\Gamma_- = \exp\left(-\sideset{}{'}\sum_{\mathbf{q}} d_{\mathbf{q}}[2 - 2\cos(\mathbf{q}(\mathbf{r}_\gamma - \mathbf{r}_\beta))]\frac{1 - \cos(\omega_{\mathbf{q}}t)}{(\hbar^2\omega_{\mathbf{q}})^2}(2N_{\mathbf{q}}(T) + 1)\right), \tag{17}$$

$$\Gamma_+ = \exp\left(-\sideset{}{'}\sum_{\mathbf{q}} d_{\mathbf{q}}[2 + 2\cos(\mathbf{q}(\mathbf{r}_\gamma - \mathbf{r}_\beta))]\frac{1 - \cos(\omega_{\mathbf{q}}t)}{(\hbar^2\omega_{\mathbf{q}})^2}(2N_{\mathbf{q}}(T) + 1)\right), \tag{18}$$

where $\mathbf{r}_\gamma$ and $\mathbf{r}_\beta$ denote the positions of the two atoms. Although the overall structure of these three decoherence terms looks very similar they behave quite differently. Let us for the moment assume that only such momenta $\mathbf{q}$ contribute considerably to the

sum for which the condition $\mathbf{q}(\mathbf{r}_\gamma - \mathbf{r}_\beta) \ll 1$ holds. This is typically the case for a temperature of $T \approx 0$ and the atoms trapped in two neighbouring lattice sites. Then, $\Gamma_- \approx 1$, which means that the decoherence for an initial state $|\psi\rangle = (|10\rangle \pm |01\rangle)/\sqrt{2}$ is strongly suppressed, because the fluctuations of the condensate happen on a length scale which is too large to resolve the distance between the two atoms. In contrast, the decay of the off-diagonal elements of the initial state $|\psi\rangle = (|11\rangle \pm |00\rangle)/\sqrt{2}$ is enhanced. These effects of sub- and superdecoherence have been predicted in Ref. [38] for a general type of qubit-environment coupling and are similar to the Dicke effect [57] well known in quantum optics. However, in our case it is not the decay rate of the excited state which is suppressed or enhanced. Instead, only the off-diagonal elements of the density matrix are affected leaving the occupation numbers unchanged.

As depicted in Fig. 2, these effects can indeed be observed for realistic experimental parameters. Figure 2(a) shows the time dependence of the three functions. Γ_- reaches its stationary state very quickly, whereas the two other functions drop exponentially to zero. The temperature dependence is shown in Fig. 2(b). Since for higher temperatures phonons with shorter wavelengths become more important, the condition $\mathbf{q}(\mathbf{r}_\gamma - \mathbf{r}_\beta) \ll 1$ is no longer fulfilled and Γ_- decreases, however considerably slower than Γ_+. The condition is also violated when the distance between the two atoms is increased, as shown in Fig. 2(c). Interestingly, the function Γ_+ shows exactly the opposite behaviour: With increasing distance, the value of the function increases as well, until it reaches the same value as Γ_-.

4.3. Implications for the quantum register

The dephasing investigated in the previous section has severe implications on the performance of a quantum register. In order to store the information two internal states $|0'\rangle$ and $|1'\rangle$ of the lattice atoms are needed, and we assume that these states do not couple to the BEC, in which case there is also no decoherence caused by the condensate coupling. However, the BEC can be used to perform a two-qubit gate between two atoms submerged into it as detailed in Ref. [37]. In short, if an atom is in state, say, $|1'\rangle$, it will be driven by a laser pulse to a state $|1\rangle$ which couples to the condensate, whereas the state $|0'\rangle$ is either unaffected or driven to a state $|0\rangle$ which does not couple to the BEC. If both atoms involved are in state $|1\rangle$ they can exchange BEC phonons which causes an additional energy shift. In the previous section, this evolution was described by the unitary $\hat{U}_{\mathrm{coh}}$, and by appropriately chosen laser pulses this operator results in a controlled-phase gate. However, due to the coupling the atoms also get entangled with the BEC, which results in dephasing after tracing out the condensate.

The influence of the dephasing on the density matrix $\hat{\varrho}_2$ is suitably expressed by using Kraus operators E_j. The super-operator Λ giving the effect of the dephasing (excluding the controlled-phase gate) can be expressed as

$$\Lambda(\hat{\varrho}_2) = \sum_{j=1}^{d} E_j \hat{\varrho}_2 E_j^\dagger \,, \tag{19}$$

where d is the dimensionality of the quantum system, here $d = 4$ for two qubits. Since the dephasing Λ commutes with the controlled-phase operation, the effect of the noisy gate is described by $\Lambda_g(\hat{\varrho}_2) = \hat{U}_{cZ} \Lambda(\hat{\varrho}_2) \hat{U}_{cZ}^\dagger = \Lambda(\hat{U}_{cZ} \hat{\varrho}_2 \hat{U}_{cZ}^\dagger)$. The Kraus operators for Λ are given in Appendix B, where we also show how the average fidelity $\langle F \rangle$ of the

noisy gate can be calculated using the explicit form of these operators. We find

$$\langle F \rangle = \frac{1}{10}(4 + 4\Gamma_0 + \Gamma_- + \Gamma_+). \tag{20}$$

From the definition of the dephasing terms it is evident that the fidelity is worse for higher interactions κ between the BEC and the lattice atoms. On the other hand, a lower interaction κ means a lower interaction strength between the two atoms and hence it takes a longer time to perform the gate. In the three-dimensional case, by choosing an arbitrary low interaction strength κ, the average gate fidelity can be brought arbitrarily close to 1, however the time to perform the gate gets arbitrarily long as well. Since there also exist other decoherence mechanisms in cold atom systems, this will eventually decrease the performance of the setup.

For concreteness, we consider the three-dimensional case where two ^{133}Cs atoms are placed in two neighbouring lattice sites with wavelength $\lambda = 790$nm. They are surrounded by a ^{23}Na BEC with a number density of $(5 \times 10^6)^3/\text{m}^3$ and an interaction strength of $g = 1.5 \times 10^{-2} E_\text{R} \lambda^3$. Here, $E_\text{R} = (2\pi\hbar)^2/2m_1\lambda^2$ is the recoil energy, with m_1 the mass of the lattice atoms and λ the wave length of the laser creating the lattice. The interspecies coupling is given by $\kappa = 1.1 \times 10^{-2} E_\text{R} \lambda^3$. In the thermodynamic limit, for $i \neq j$ and $\xi \gg x_0$ the mediated interaction is $V_{i,j} = \kappa^2 \xi \exp(-\sqrt{2}|i - j|a/\xi)/\pi g\xi^3|i - j|a$, where a is the distance between two neighbouring lattice sites. This leads to the (minimal) gate time $t_g = \hbar\pi/V_{1,2} = 40$ms [37], where the gate fidelity is given by $\langle F \rangle = 0.99$. For getting the last result, we used the approximations $\Gamma_x \geq \exp(-c_x\kappa^2/\sqrt{2}\pi^2 g^2 n_0\xi^3)$, which hold in the thermodynamic limit, $T = 0$, $\xi \gg x_0$, and where $c_0 = 1$, $c_- = 2$, and $c_+ = 4$.

For the case of two or one spatial dimensions, the interaction is in general larger and thus the expected gate times shorter. However, the fidelities decrease much faster than for three dimensions, and all of our numerical tests showed that for the same gate times the three-dimensional fidelities were always better than the ones achieved in lower dimensions. Although this restricts the applicability of this setup for quantum information purposes, the scheme can still be used for probing the interaction strength which is mediated by the condensate, simply by measuring the phase differences for varying interaction times.

5. Clustering of the lattice atoms

If the lattice is not uniformly filled with atoms but the filling ranges somewhere between zero and one atom per lattice site, the mediated interaction has an important impact on the spatial distribution of the atoms. For low enough temperatures, it will lead to atom clusters. To observe the clustering of the atoms we have to allow for a weak hopping $J \ll |V_{1,2}|, |U|,\S$, because otherwise the atom distribution remains stationary. We can assume that the perturbation due to the hopping does not change the interaction potential $V_{i,j}$ derived from the exact solution, which is in agreement with our earlier findings [34]. The hopping energy can furthermore be neglected compared to the interaction potential, such that the weak hopping leads only to a re-arrangement of the atoms, which is similar to the treatment of ad-atoms on crystal

---

§ In the assumed homogeneous setup the value $V_{1,2}$ corresponds to the mediated interaction between two nearest neighbours and $V_{1,1}$ to the mediated on-site interaction.

surfaces [40]. The Hamiltonian for this situation is given by

$$\hat{H}_{\mathrm{cl}} = \frac{U}{2} \sum_j \hat{n}_j(\hat{n}_j - 1) - \sum_{i,j} V_{i,j} \hat{n}_i \hat{n}_j \,. \tag{21}$$

The mediated on-site interaction $V_{1,1}$, which in our case is always attractive, cf. equation (13), might overcompensate the on-site interaction U, i.e., $U + V_{1,1} < 0$. If this happens, all the atoms can aggregate in a single lattice site, which will inevitably lead to three-body losses. We therefore assume that the repulsive on-site interaction U is large enough such that states with more than one atom in a single lattice site can be neglected, i.e., $U + V_{1,1} \gg J$. For the parameters used below (see captions of Figs. 3 and 4) the mediated on-site interaction is given by $V_{1,1} = -0.03E_{\mathrm{R}}$ in one dimension and $V_{1,1} = -0.08E_{\mathrm{R}}$ in two. Since we require a deep lattice for the hopping J to be small, a sufficiently high U can easily be achieved. For a reasonably deep lattice of $15E_{\mathrm{R}}$ and perpendicular confinement of $35E_{\mathrm{R}}$, the interaction strength is on the order of $U \approx 0.4E_{\mathrm{R}}$ for a one-dimensional lattice and $U \approx 0.3E_{\mathrm{R}}$ for two dimensions and thus sufficiently high to overcome the induced on-site attractive interaction. The repulsive interaction strength corresponds to a temperature of $U/k_{\mathrm{B}} = 150$nK in one dimension ($U/k_{\mathrm{B}} = 130$nK in two dimensions), such that neglecting states with more than one atom per lattice site is well-justified for the temperature regime considered, see below. With these assumptions, the ground state for the lattice system consists of a cluster where all the atoms are located in neighbouring lattice sites. We note that this also holds if the lattice is loaded with spin-polarised fermions, in which case the Pauli exclusion principle ensures that there is never more than one atom in each lattice site. The restriction to a maximum of one atom per lattice site and ignoring interactions beyond nearest neighbours makes it also possible to map the system to an Ising model by using the correspondence $\hat{n}_j = (1 + \hat{s}_j)/2$, which gives

$$\hat{H}_{\mathrm{cl}} = -\frac{V_{1,2}}{4} \sum_{\langle i,j \rangle} \hat{s}_i \hat{s}_j - V_{1,2} \sum_j \hat{s}_j \,, \tag{22}$$

where a constant term has been neglected. We will make use of this correspondence shortly when we compare our results to analytical ones found for the Ising model in two dimensions.

In an experiment, the lattice atoms will have a finite temperature T, which leads to a breaking up of the ground state into smaller clusters, reflecting the increased average energy. It is therefore important to investigate at which temperatures the clustering can be observed. To this end, we simulated the lattice system using the well-established Metropolis algorithm [58, 59], which is often used in the simulation of classical lattice spin and lattice gas models when the kinetic energy can be neglected compared to the interaction energies. For a one-dimensional lattice, the averaged number of clusters‖ for different temperatures is shown in Fig. 3(a). For temperatures above $T = 7$nK the number of clusters does not change very much with the temperature and roughly 110 clusters exist, which shows that most of the atoms do not have nearest neighbours. A drastic reduction of the cluster number only occurs for $T < 7$nK, such that the number of clusters finally reaches $N_{\mathrm{c}} = 1$ for $T \approx 0$. A method to achieve such low temperatures of below 7 nK has been proposed, where the surrounding BEC is first used for dark-state cooling [32, 33].

The numerical data in Fig. 3 is compared to an analytical result derived in the thermodynamic limit, where the number of lattice sites M goes to infinity

---

‖ Note that a single atom without nearest neighbours is also considered to constitute a cluster.
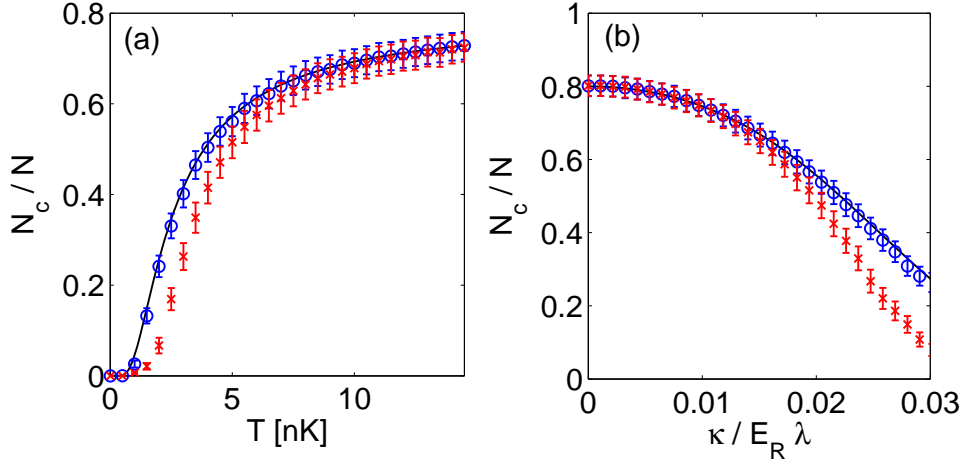
Figure 3. Normalised cluster number N_c/N versus (a) temperature of the one-dimensional lattice gas and (b) coupling to the BEC. The solid line shows the analytical estimate given in Eq. (23), results from numerical calculations only taking the nearest neighbour interaction into account are marked by 'o' and numerical results including the full interaction potential are marked by 'x'. The algorithm was run for 10^8 steps after which an equilibrium state is reached. Then, another 5×10^7 steps were done and after every 1000 steps the number of clusters was calculated. Error bars show one standard deviation derived from averaging over those results. The lattice with wavelength $\lambda = 790$nm consists of $M = 800$ lattice sites filled with $N = 160$ ^{41}K atoms. The surrounding BEC was assumed to consist of ^{87}Rb atoms with a linear number density of $n = 5 \times 10^6$/m and a coupling $g/E_R\lambda = 1.1 \times 10^{-2}$. In (a), the interspecies coupling is given by $\kappa/E_R\lambda = 2.5 \times 10^{-2}$, whereas in (b) the temperature is fixed to $T = 3$nK. Periodic boundary conditions were assumed.

whilst keeping the filling fraction N/M constant, and only taking nearest-neighbour interactions into account [60]. In this case, the normalised number of clusters N_c/N is given by

$$\frac{N_c}{N} = \frac{M}{N} \frac{\sqrt{1 + 4(M-N)N \left[\exp(2|V_{1,2}|/k_B T) - 1\right]/M^2} - 1}{2[\exp(2|V_{1,2}|/k_B T) - 1]} , \quad (23)$$

where k_B is Boltzmann's constant. Our calculations show that the numerical results taking only the nearest neighbour term of the interaction into account is in excellent agreement with the result for the thermodynamic limit. We furthermore observe that the number of clusters for the full interaction potential is for low temperatures considerably smaller than for the truncated one, which indicates that the interaction terms beyond nearest neighbours make the clusters more stable. This gets also apparent when the temperature is fixed and the number of clusters is calculated for different coupling strengths κ, as shown in Fig. 3(b). For small κ the interaction beyond nearest neighbours is still quite weak and does not change the number of clusters significantly, whereas for stronger coupling κ, interaction terms beyond nearest neighbours are considerable, reflected in a smaller number of clusters or, equivalently, in a larger average cluster size.

The situation gets more interesting if we consider a two-dimensional lattice. For $T \approx 0$, the atoms aggregate in an "island" and for increasing temperature parts of
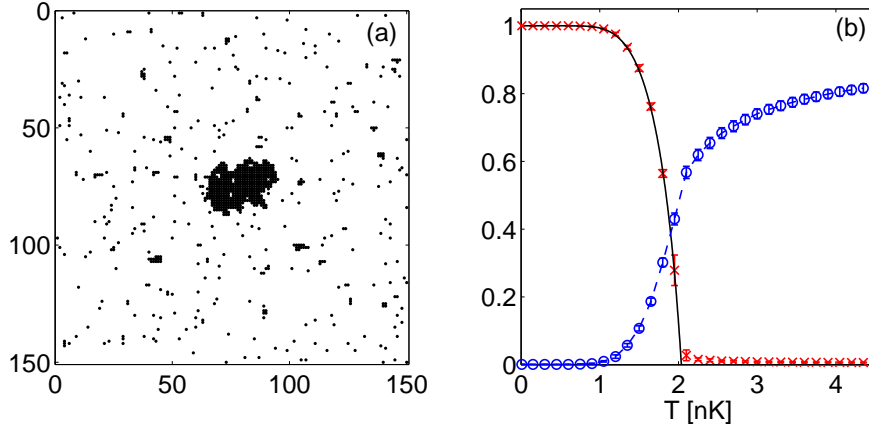
Figure 4. (a) Distribution of the atoms in a homogenous two-dimensional lattice with periodic boundary conditions and a temperature of $T = 1.8$nK. A macroscopic island is clearly visible. (b) Normalised size of the largest cluster N_I/N versus temperature of the lattice gas for a two-dimensional system (marked by 'x') and normalised number of clusters N_c/N (marked by 'o'). The solid line shows the analytical expression given in Eq. (24), the dashed line is a guide to the eye. Error bars show one standard deviation derived from averaging over several runs. The lattice with wavelength $\lambda = 790$nm consists of $M = 150 \times 150$ lattice sites filled with 900 ^{41}K atoms. The surrounding BEC was assumed to consist of ^{87}Rb atoms with a number density of $n = 25 \times 10^{12}/\mathrm{m}^2$ and a coupling $g/E_\mathrm{R}\lambda^2 = 5.1 \times 10^{-3}$. The interspecies coupling is given by $\kappa/E_\mathrm{R}\lambda^2 = 1.87 \times 10^{-2}$.

this island break away, see Fig. 4(a). We have calculated the size of the largest cluster (i.e. the number N_I of atoms constituting the island) numerically, only taking nearest neighbour interactions into account. This will give a lower bound for the temperature below which the formation of the island can be observed. The results are shown in Fig. 4(b). For very low temperatures, all the atoms are contained in a single cluster. This largest cluster gets smaller with increasing temperature and shows a pronounced transition at a temperature of $T \approx 2$nK, above which the system mainly consists out of many small clusters. It has been shown in Ref. [61], that the normalised size N_I/N of the island in the thermodynamic limit and only taking nearest neighbour interactions into accout behaves as

$$\frac{N_I}{N} = \frac{(1 + N_0)(N_0 - N_r)}{2N_0(1 - N_r)} \,. \tag{24}$$

Here, $N_0 = \{1 - [\sinh(2J_\mathrm{s}/k_\mathrm{B}T)]^{-4}\}^{1/8}$, and $J_\mathrm{s} = |V_{1,2}|/4$. For this formula to be valid we further require a filling of $N/M \leq 1/2$, such that $N_r = 1 - 2N/M \geq 0$, and above the transition temperature T_I where N_I/M hits zero for the first time, the function has to be set to zero, since for this temperature the normalised size of the largest island vanishes in the thermodynamic limit. Our Monte-Carlo results are in excellent agreement with Eq. (24), deviations above the transition temperature are due to finite size effects. We note that a higher transition temperature T_I can be achieved by increasing the interaction strength $V_{i,j}$ or by loading more atoms into the lattice. We find $k_\mathrm{B}T_I = 2J_\mathrm{s}/\mathrm{arsinh}\left[1/\sqrt[4]{1 - N_r^8}\right]$, which yields for the chosen values
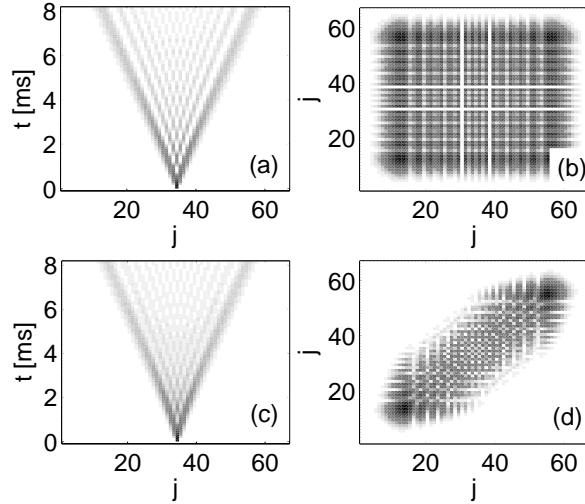
Figure 5. (a) and (c) time evolution of the atom density. (b) and (d) graphical representation of the absolute values of the density matrix for the final time step $t = 8.2$ms shown in (a) and (c). Darker colour corresponds to a higher numerical value. For the examples shown we have assumed a ^{41}K atom in an optical lattice with wave length $\lambda = 790$nm, and a hopping of $J = 0.03E_\mathrm{R}$. The BEC consists of ^{87}Rb atoms with a density of $n_0 = 5 \times 10^6$/m and a coupling of $g/E_\mathrm{R}\lambda = 1.1 \times 10^{-2}$. The temperature is given by $T = 100$nK. The interspecies coupling for case (a) and (b) was assumed to be $\kappa = 0$, whereas for (c) and (d) it was $\kappa/E_\mathrm{R}\lambda = 1.94 \times 10^{-2}$. For recent experiments on these mixtures, see Refs. [22, 62].

(see caption of Fig. 4) and $N_r \to 0$ a value of $T_I = 2.34$nK.

6. Transport properties of the impurity atoms

In this section, we use the QME to investigate the behaviour of the lattice system for a hopping $J \gg E_p$. In general, an analytical solution of the QME is no longer possible, and the dynamics has to be calculated numerically. Let us consider the simple case of one atom initially localised in a single lattice site. With vanishing coupling to the condensate, the atom will spread across the lattice coherently in a wavelike motion, as shown in Fig. 5(a). The interference fringes between the two wave fronts are clearly visible. The coherent nature of the evolution is also reflected in the density matrix, where all off-diagonal elements have their maximum possible value, compare Fig. 5(b). The situation changes when the coupling to the condensate is increased, as shown in Fig. 5(c). The wave-fronts still exist, however the region in between no longer exhibits clear interference patterns, which are washed out instead. This implies that the coherent nature of the evolution is impaired, which is also supported by the density matrix, see Fig. 5(d). The off-diagonal elements are clearly suppressed, which confirms the incoherent character.

The motion of the atom in the lattice can be explained by the coexistence of wavelike, coherent evolution responsible for the two wave-fronts, and a diffusive, incoherent evolution. The diffusive motion stems from the decay of the off-site
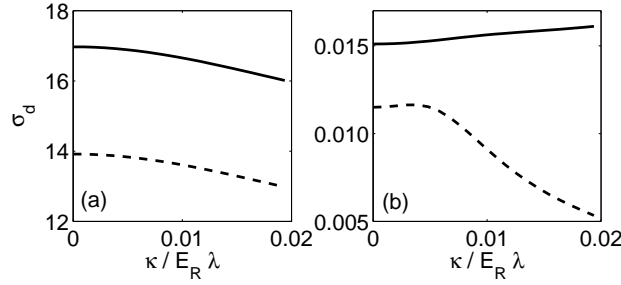
Figure 6. (a) Standard deviation of the density distribution after an evolution time of $t = 6.7$ms (dashed line) and $t = 8.2$ms (solid line). (b) Average density $\bar{p}$ (solid line) and standard deviation p_d (dashed line). Apart from the interspecies coupling κ, all the parameters are as in Fig. 5.

elements in the density matrix, which destroys the memory of the atom and causes it to perform a random walk, leading to the washing out of the interference effects between the two wave fronts. To investigate the time evolution more quantitatively, we calculate the standard deviation σ_d of the atom density distribution at a time t, given by $\sigma_d = \sum_j p_j (j - j_0)^2$, where j labels the lattice sites, p_j is the probability of finding the atom at lattice site j, and j_0 is the initial lattice site of the atom at $t = 0$. Figure 6(a) shows that for an increasing coupling to the condensate this standard deviation σ_d decreases. This stems from the fact that the hopping is reduced due to the coupling between the lattice atoms and the phonons of the BEC, which has also been observed in Ref. [34].

Taking one standard deviation to either side of j_0 defines a suitable interval I between the two wave fronts to investigate the diffusive character of the motion. For this interval, we calculate the average atom density $\bar{p} = \sum_{j \in I} p_j / 2\sigma_d$ and the standard deviation of the density distribution $p_d = \sum_{j \in I} (p_j - \bar{p})^2 / 2\sigma_d$. For the coherent case, we expect that this standard deviation is on the order of the average density $\bar{p}$ due to the interference patterns, whereas for the incoherent case the standard deviation should be much lower than the average density due to the more homogenous spread of the atom between the two wave fronts. These expectations are confirmed by our findings shown in Fig. 6(b). We observe that the average density between the two wave fronts $\bar{p}$ moderately increases with increasing interspecies coupling. The standard deviation of this density p_d stays first approximately constant with increasing κ, indicating a regime where the evolution can still be considered to be coherent, but then for $\kappa > 5 \times 10^{-3} E_R \lambda$ drops off considerably, caused by the increased loss of coherence.

The QME describes the lattice atoms well as long as only dephasing has to be taken into account and energy exchange with the BEC can be neglected. This is consistent with the approximations we have used to derive the QME: It was assumed that $Ja/\hbar \ll c$, which means that the atoms move slower than the critical velocity of the BEC. Then, according to the Landau criterion for superfluidity, no energy exchange is possible with a single phonon process, and higher order phonon processes are not included into the QME.

This gets especially apparent when we try to describe the decay of Bloch oscillations with the QME. Let us assume a Stark potential $\hat{H}_s = K \sum_j j \hat{n}_j$ is applied to the one-dimensional optical lattice. For one particle initially located in a
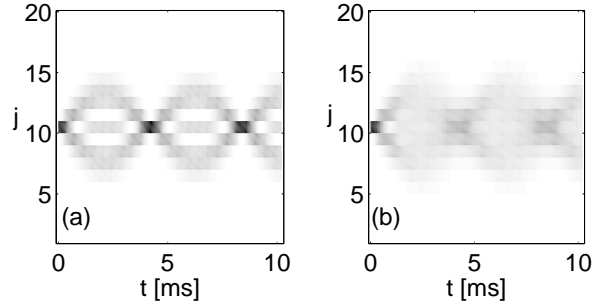
Figure 7. Bloch oscillations in an optical lattice submerged into a BEC of ^{87}Rb atoms with a density of $n_0 = 5 \times 10^6$/m, a coupling of $g/E_R\lambda = 1.1 \times 10^{-2}$ and a temperature of $T = 75$nK. The ^{41}K atom is trapped in a lattice with wavelength $\lambda = 790$nm and has a hopping rate of $J = 0.03E_R$. The strength of the Stark potential is given by $K/\hbar = 1.5$kHz. The interspecies coupling is given by (a) $\kappa = 0$ and (b) $\kappa/E_R\lambda = 1.6 \times 10^{-2}$.

single lattice site and not coupling to the BEC, we expect breathing oscillations with frequency $\omega_B = K/\hbar$ and width $4J_a|\sin(\omega_B t/2)|/K$ [63]. This is shown in Fig. 7(a). When the atom couples to the BEC, it can dissipate energy into the condensate modes and one expects that the atom can "fall down" the tilted lattice, causing a net current. When using the QME to describe the dynamics this is, however, not the case. Instead, the Bloch oscillations only get washed out, but the mean position of the atom remains unchanged, as shown in Fig. 7(b). This is in agreement with our expectations and with other attempts to describe the system with a simple Master Equation approach [64]. An alternative way based on a generalised master equation, which includes the coupling of phonons to the hopping term, has been devised to describe the occurrence of an atomic net current. Details will be given elsewhere [65].

Another way to observe the net current is given by solving the complete dynamics of the atom and the surrounding BEC numerically. For this, the BEC has to be discretised, which is equivalent to assuming that it is trapped in an optical lattice with appropriately chosen hopping and interaction constants [66]. The Hamiltonian describing the system is then given by

$$\hat{H} = \hat{H}_L - J_b \sum_{\langle i,j \rangle} \hat{\beta}_i^\dagger \hat{\beta}_j + \frac{U_b}{2} \sum_j \hat{\beta}_j^\dagger \hat{\beta}_j^\dagger \hat{\beta}_j \hat{\beta}_j + U_i \sum_j \hat{\beta}_j^\dagger \hat{\beta}_j \hat{a}_j^\dagger \hat{a}_j \,, \tag{25}$$

with $\hat{\beta}_j^\dagger$ ($\hat{\beta}_j$) an operator that creates (annihilates) a boson in lattice site j, U_b the on-site interaction strength and J_b the hopping matrix element of the BEC atoms, and U_i the interspecies interaction strength. The time evolution of this Hamiltonian including the BEC and a single atom in the lattice is performed numerically by using the time evolving block decimation (TEBD) algorithm [67–69]. The resulting density distribution of the lattice atom initially placed in a single lattice site and evolved for one Bloch period is shown in Fig. 8(a). For a weak interaction strength $U_i \ll J_b$ the surrounding BEC atoms hardly affect the dynamics of the lattice atom and after one cycle it ends up in its original lattice site again. For increased interaction the lattice atom is able to dissipate more and more energy to the BEC and to drift towards lattice sites with a lower potential energy, which leads to a net current. This is illustrated in Fig. 8(b), where a competition between Bloch oscillation and net current is clearly
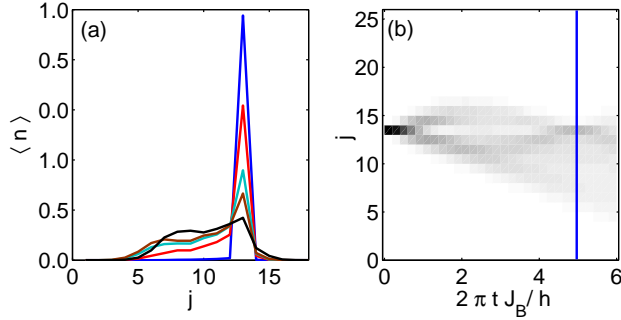
Figure 8. (a) Decay of Bloch oscillations and occurrence of a net current. Shown are the density distributions of one atom initially localised in lattice site 13 after a time evolution of $t = 2\pi/\omega_B$ for different interaction strengths ranging from $U_i = \{0.1; 0.5; 0.8; 1; 2\}J_b$ (top to bottom line in lattice site 13). The dynamics of the lattice atom and the BEC consisting of 25 atoms was calculated in an optical lattice with 25 lattice sites using the TEBD algorithm. We used $J_a = J_b$, $U_b = 0.5J_b$, $K = 1.25J_b$, $T = 0$. (b) Time evolution of the density distribution for one lattice atom with $U_i = J_b$. The coexistence of Bloch oscillations and a current is visible. The vertical line indicates the time where the densities of (a) are taken.

visible. The current can be measured either directly or after a time of flight expansion of the lattice atoms as detailed in Ref. [70].

7. Conclusion

In the present paper we have investigated the behaviour of an optical lattice system immersed into a BEC. To this end, we have derived a quantum master equation which describes the time evolution of the lattice atoms. For the case of fixed impurities, the lattice system represents a quantum register and the internal states of the atoms represent the states of the qubit. We have derived an exact solution for this system which is reproduced by the QME. We found that an interaction between the lattice atoms is mediated by the condensate and that the coupling to the phonon modes of the BEC causes a dephasing of the lattice atoms, i.e., of the qubits they represent. This dephasing can be used to probe the properties of the BEC with different sensitivity.

The interaction between the lattice atoms leads to a clustering process at low enough temperatures. In contrast to on-site clusters, which are prone to three-body losses, the clustering in our case is caused by the off-site interaction terms. We have simulated the clustering process using the Metropolis algorithm and compared our results with analytical ones originally found for spin systems or ad-atoms on a crystal surface. Our findings indicate that for realistic experimental parameters the clustering process occurs at temperatures of about 5nK and is observable with near-future experimental techniques.

We also investigated the transport properties of the lattice atoms subject to the BEC coupling. We found that the lattice atoms undergo a crossover from coherent to incoherent evolution when the interaction to the condensate is increased. This process is indicated by a washing out of the typical interference fringes in the density distribution and by vanishing off-diagonal elements in the one-particle density matrix.

However, due to the approximations necessary to derive the QME, it does not include dissipation of energy to the BEC. This process is a vital effect to describe the decay of Bloch oscillations in a tilted lattice. More work is necessary to include this effect into a master equation description.

Acknowledgments

Appendix A. Derivation of the QME

The details of deriving the QME are given in this Appendix. Our starting point is the Liouville-von Neumann equation for the total density operator $\hat{\varrho}(t)$,

$$i\hbar\partial_t\hat{\varrho}(t) = [\hat{H}, \hat{\varrho}(t)]. \tag{A.1}$$

For a general operator $\hat{O}$ in the Schrödinger picture we define the corresponding operator $\tilde{O}(t)$ in the interaction picture by

$$\tilde{O}(t) = e^{i(\hat{H}_B+\hat{H}_L)t/\hbar}\,\hat{O}\,e^{-i(\hat{H}_B+\hat{H}_L)t/\hbar}. \tag{A.2}$$

With this, the Liouville-von Neumann equation changes to

$$i\hbar\partial_t\tilde{\varrho}(t) = [\tilde{H}_I(t), \tilde{\varrho}(t)]. \tag{A.3}$$

If there was no interaction between the lattice atoms and the BEC before a time $t_0 = 0$, it is reasonable to assume that the density operator at time t_0 is described by $\hat{\varrho}(0) = \hat{\varrho}_L(0)\otimes\hat{\varrho}_B(0)$, i.e., at time t_0 there are no correlations present between the BEC and the lattice atoms. Here, $\hat{\varrho}_L(0)$ and $\hat{\varrho}_B(0)$ are the initial density operators of the lattice system and the BEC, respectively. We furthermore assume that at t_0 the BEC is in a thermal state with temperature T. Integrating the Liouville-von Neumann equation, substituting it into itself and using the definition of $\tilde{H}_I(t)$, we find after applying the Born approximation and taking the trace over the BEC variables [52]

$$\partial_t\tilde{\varrho}_L(t) = -\frac{1}{\hbar^2}\int_0^t dt' \sum_{\mathbf{q}}{}' \sum_{l,l'} \{[\tilde{n}_l(t)\tilde{n}_{l'}(t')\tilde{\varrho}_L(t') - \tilde{n}_{l'}(t')\tilde{\varrho}_L(t')\tilde{n}_l(t)]C_{\mathbf{q},l,l'}(t-t')$$
$$+ [\tilde{\varrho}_L(t')\tilde{n}_{l'}(t')\tilde{n}_l(t) - \tilde{n}_l(t)\tilde{\varrho}_L(t')\tilde{n}_{l'}(t')]C^*_{\mathbf{q},l,l'}(t-t')\}, \tag{A.4}$$

with

$$C_{\mathbf{q},l,l'}(t-t') = F_{\mathbf{q},l}F^*_{\mathbf{q},l'}(1+N_{\mathbf{q}}(T))\,e^{-i\omega_{\mathbf{q}}(t-t')} + F^*_{\mathbf{q},l}F_{\mathbf{q},l'}N_{\mathbf{q}}(T)\,e^{i\omega_{\mathbf{q}}(t-t')}. \tag{A.5}$$

Under the assumption that the sound velocity of the condensate, $c \sim \sqrt{gn_0/m_b}$, is larger than the typical hopping speed of the atoms, $c \gg Ja/\hbar$, the dynamics of the BEC is much faster than the typical dynamics of the lattice atoms and we perform the Markov-approximation by replacing $\tilde{\varrho}_L(t') \rightarrow \tilde{\varrho}_L(t)$ and $\tilde{n}_l(t') \rightarrow \tilde{n}_l(t)$. After calculating the time integral and transforming back into the Schrödinger picture we finally arrive at Eq. (9).

Appendix B. Kraus operators for the two-qubit dephasing

Here, we give explicit formulas for the Kraus operators describing the operator Λ given by $\Lambda(\hat{\varrho}_\mathbf{2}) = \hat{U}^\dagger_{cZ}\Lambda_g(\hat{\varrho}_\mathbf{2})\hat{U}_{cZ}$. We find

$$E_1 = \sqrt{(1 + 2\Gamma_0 + \Gamma_+)/4}\,\mathbf{1}_4\,, \tag{B.1}$$

$$E_2 = \sqrt{(1 - 2\Gamma_0 + \Gamma_+)/4}\,\sigma_z \otimes \sigma_z\,, \tag{B.2}$$

$$E_3 = \sqrt{(1 - \Gamma_-)/4}\,\sigma_z \otimes \mathbf{1}_2\,, \tag{B.3}$$

$$E_4 = \sqrt{(1 - \Gamma_-)/4}\,\mathbf{1}_2 \otimes \sigma_z\,, \tag{B.4}$$

$$E_5 = \sqrt{(\Gamma_- - \Gamma_+)/4}\,\mathrm{diag}(-1, 1, 1, 1)\,, \tag{B.5}$$

$$E_6 = \sqrt{(\Gamma_- - \Gamma_+)/4}\,\mathrm{diag}(1, 1, 1, -1)\,, \tag{B.6}$$

and all other Kraus operators are zero. Here, $\mathbf{1}_n$ is the $n \times n$ unit matrix, σ_z is the Pauli z matrix, and diag is a diagonal matrix with the entries on the diagonal given as the argument.

With the knowledge of the Kraus operators the average fidelity $\langle F \rangle$ of the gate is calculated as follows. We first note that the fidelity F of the noisy operation Λ_g with respect to the perfect (i.e., noise-free) operation $\hat{U}_{cZ}$ on a special input state $|\psi\rangle$ is defined by

$$F(\psi) = \langle\psi|\hat{U}^\dagger_{cZ}\,\Lambda_g\{|\psi\rangle\langle\psi|\}\,\hat{U}_{cZ}|\psi\rangle\,. \tag{B.7}$$

By taking the average over all possible input states the overall performance of the gate operation can be estimated. It has been shown [71, 72] that the average fidelity is given by

$$\langle F \rangle = \int_{S^{2d-2}} F(\psi)\,\mathrm{d}\psi = \frac{1}{d(d+1)}\left(\sum_{j=1}^{d^2}|\,\mathrm{tr}(E_j)|^2 + d\right)\,, \tag{B.8}$$

where the integral is taken over the unit sphere S^{2d-2} embedded in $2d-1$-dimensional real space, which is isomorphic to the d-dimensional complex space after eliminating a global phase, and $\mathrm{d}\psi$ is the normalised measure over the sphere, also know as Haar measure. With this formula and the explicit form of the Kraus operators the calculation of the average fidelity Eq. (20) is straight forward.

We note that the Kraus operators for a coupling to independent reservoirs are given by replacing $\Gamma_- = \Gamma_+ = (\Gamma_0)^2$. This gives an average fidelity of $\langle F_{\mathrm{ind}}\rangle = (2 + 2\Gamma_0 + (\Gamma_0)^2)/5$. Hence the coupling to the BEC reservoir is worse than the one to independent reservoirs if $\Gamma_+ + \Gamma_- < 2(\Gamma_0)^2$.

References

[1] Lewenstein, M., Sanpera, A., Ahufinger, V., Damski, B., Sen, A., and Sen, U. Ultracold atomic gases in optical lattices: mimicking condensed matter physics and beyond. *Advances in Physics* **56**, 243 (2007).

[2] Jaksch, D., Bruder, C., Cirac, J. I., Gardiner, C. W., and Zoller, P. Cold bosonic atoms in optical lattices. *Phys. Rev. Lett.* **81**, 3108 (1998).

[3] Jaksch, D. and Zoller, P. The cold atom Hubbard toolbox. *Annals of Physics (NY)* **315**, 52 (2005).

[4] Sørensen, A. and Mølmer, K. Spin-spin interaction and spin squeezing in an optical lattice. *Phys. Rev. Lett.* **83**, 2274 (1999).

[5] Duan, L.-M., Demler, E., and Lukin, M. D. Controlling spin exchange interactions of ultracold atoms in optical lattices. *Phys. Rev. Lett.* **91**, 090402 (2003).

[6] Hofstetter, W., Cirac, J. I., Zoller, P., Demler, E., and Lukin, M. D. High-temperature superfluidity of fermionic atoms in optical lattices. *Phys. Rev. Lett.* **89**, 220407 (2002).

[7] Klein, A. and Jaksch, D. Simulating high-temperature superconductivity model Hamiltonians with atoms in optical lattices. *Phys. Rev. A* **73**, 053613 (2006).

[8] Jaksch, D. and Zoller, P. Creation of effective magnetic fields in optical lattices: the Hofstadter butterfly for cold neutral atoms. *New J. Phys.* **5**, 56 (2003).

[9] Juzeliūnas, G. and Öhberg, P. Slow light in degenerate Fermi gases. *Phys. Rev. Lett.* **93**, 033602 (2004).

[10] Juzeliūnas, G., Öhberg, P., Ruseckas, J., and Klein, A. Effective magnetic fields in degenerate atomic gases induced by light beams with orbital angular momenta. *Phys. Rev. A* **71**, 053614 (2005).

[11] Juzeliūnas, G., Ruseckas, J., Öhberg, P., and Fleischhauer, M. Light induced effective magnetic fields for ultra-cold atoms in planar geometries. *Phys. Rev. A* **73**, 025602 (2006).

[12] Mueller, E. J. Artificial electromagnetism for neutral atoms: Escher staircase and Laughlin liquids. *Phys. Rev. A* **70**, 041603(R) (2004).

[13] Sørensen, A. S., Demler, E., and Lukin, M. D. Fractional quantum Hall states of atoms in optical lattices. *Phys. Rev. Lett.* **94**, 086803 (2005).

[14] Osterloh, K., Baig, M., Santos, L., Zoller, P., and Lewenstein, M. Cold atoms in non-abelian gauge potentials: From the Hofstadter moth to lattice gauge theory. *Phys. Rev. Lett.* **95**, 010403 (2005).

[15] Ruseckas, J., Juzeliūnas, G., Öhberg, P., and Fleischhauer, M. Non-abelian gauge potentials for ultracold atoms with degenerate dark states. *Phys. Rev. Lett.* **95**, 010404 (2005).

[16] Palmer, R. and Jaksch, D. High field fractional quantum Hall effect in optical lattices. *Phys. Rev. Lett.* **96**, 180407 (2006).

[17] Bloch, I. Ultracold quantum gases in optical lattices. *Nat. Phys.* **1**, 23 (2005).

[18] Greiner, M., Mandel, O., Esslinger, T., Hänsch, T. W., and Bloch, I. Quantum phase transition from a superfluid to a mott insulator in a gas of ultracold atoms. *Nature (London)* **415**, 39 (2002).

[19] Greiner, M., Mandel, O., Hänsch, T. W., and Bloch, I. Collapse and revival of the matter wave field of a Bose-Einstein condensate. *Nature (London)* **419**, 51 (2002).

[20] Günter, K., Stöferle, T., Moritz, H., Köhl, M., and Esslinger, T. Bose-Fermi mixtures in a three-dimensional optical lattice. *Phys. Rev. Lett.* **96**, 180402 (2006).

[21] Ospelkaus, S., Ospelkaus, C., Wille, O., Succo, M., Ernst, P., Sengstock, K., and Bongs, K. Localization of bosonic atoms by fermionic impurities in a three-dimensional optical lattice. *Phys. Rev. Lett.* **96**, 180403 (2006).

[22] Catani, J., Sarlo, L. D., Barontini, G., and Inguscio, F. M. M. Degenerate Bose-Bose mixture in a 3D optical lattice. *arXiv:0706.2781v1* (2007).

[23] Tung, S., Schweikhard, V., and Cornell, E. A. Observation of vortex pinning in Bose-Einstein condensates. *Phys. Rev. Lett.* **97**, 240402 (2006).

[24] Winkler, K., Thalhammer, G., Lang, F., Grimm, R., Hecker Denschlag, J., Daley, A. J., Kantian, A., Büchler, H. P., and Zoller, P. Repulsively bound atom pairs in an optical lattice. *Nature (London)* **441**, 853 (2006).

[25] Mandel, O., Greiner, M., Widera, A., Rom, T., Hänsch, T. W., and Bloch, I. Controlled collisions for multi-particle entanglement of optically trapped atoms. *Nature (London)* **425**, 937 (2003).

[26] Mandel, O., Greiner, M., Widera, A., Rom, T., Hänsch, T. W., and Bloch, I. Coherent transport of neutral atoms in spin-dependent optical lattice potentials. *Phys. Rev. Lett.* **91**, 010407 (2003).

[27] Mathey, L., Wang, D.-W., Hofstetter, W., Lukin, M. D., and Demler, E. Luttinger liquid of polarons in one-dimensional boson-fermion mixtures. *Phys. Rev. Lett.* **93**, 120404 (2004).

[28] Pazy, E. and Vardi, A. Holstein model and Peierls instability in one-dimensional boson-fermion lattice gases. *Phys. Rev. A* **72**, 033609 (2005).

[29] Lewenstein, M., Santos, L., Baranov, M. A., and Fehrmann, H. Atomic Bose-Fermi mixtures in an optical lattice. *Phys. Rev. Lett.* **92**, 050401 (2004).

[30] Büchler, H. P. and Blatter, G. Supersolid versus phase separation in atomic Bose-Fermi mixtures. *Phys. Rev. Lett.* **91**(13), 130404 Sep (2003).

[31] LeBlanc, L. J. and Thywissen, J. H. Species-specific optical lattices. *Phys. Rev. A* **75**, 053612 (2007).

[32] Griessner, A., Daley, A. J., Clark, S. R., Jaksch, D., and Zoller, P. Dark-state cooling of atoms by superfluid immersion. *Phys. Rev. Lett.* **97**, 220403 (2006).

[33] Griessner, A., Daley, A. J., Clark, S. R., Jaksch, D., and Zoller, P. Dissipative dynamics of

atomic Hubbard models coupled to a phonon bath: dark state cooling of atoms within a Bloch band of an optical lattice. *New J. Phys.* **9**, 44 (2007).

[34] Bruderer, M., Klein, A., Clark, S. R., and Jaksch, D. Polaron physics in optical lattices. *Phys. Rev. A* **76**, 011605(R) (2007).

[35] Mahan, G. D. *Many-Particle Physics*. Kluwer Academic, New York, third edition, (2000).

[36] Bardeen, J., Baym, G., and Pines, D. Effective interaction of He^3 atoms in dilute solutions of He^3 in He^4 at low temperature. *Phys. Rev.* **156**, 207 (1967).

[37] Klein, A. and Fleischhauer, M. Interaction of impurity atoms in Bose-Einstein condensates. *Phys. Rev. A* **71**, 033605 (2005).

[38] Palma, G. M., Suominen, K.-A., and Ekert, A. K. Quantum computers and dissipation. *Proc. R. Soc. Lond. A* **452**, 567 (1996).

[39] Bruderer, M. and Jaksch, D. Probing BEC phase fluctuations with atomic quantum dots. *New J. Phys.* **8**, 87 (2006).

[40] Jensen, P. Growth of nanostructures by cluster deposition: Experiments and simple models. *Rev. Mod. Phys.* **71**, 1695 (1999).

[41] Öhberg, P., Surkov, E. L., Tittonen, I., Stenholm, S., Wilkens, M., and Shlyapnikov, G. V. Low-energy elementary excitations of a trapped Bose-condensed gas. *Phys. Rev. A* **56**, R3346 (1997).

[42] Bloch, I., Dalibard, J., and Zwerger, W. Many-body physics with ultracold gases. *arXiv:0704.3011v1 [cond-mat.other]* (2007).

[43] Theis, M., Thalhammer, G., Winkler, K., Hellwig, M., Ruff, G., Grimm, R., and Hecker Denschlag, J. Tuning the scattering length with an optically induced Feshbach resonance. *Phys. Rev. Lett.* **93**, 123001 (2004).

[44] Schrader, D., Dotsenko, I., Khudaverdyan, M., Miroshnychenko, Y., Rauschenbeutel, A., and Meschede, D. Neutral atom quantum register. *Phys. Rev. Lett.* **93**, 150501 (2004).

[45] Scheunemann, R., Cataliotti, F. S., Hänsch, T. W., and Weitz, M. Resolving and addressing atoms in individual sites of a Co_2-laser optical lattice. *Phys. Rev. A* **62**, 051801(R) (2000).

[46] Miroshnychenko, Y., Alt, W., Dotsenko, I., Förster, L., Khudaverdyan, M., Meschede, D., Schrader, D., and Rauschenbeutel, A. An atom-sorting machine. *Nature (London)* **442**, 151 (2006).

[47] Miroshnychenko, Y., Alt, W., Dotsenko, I., Förster, L., Khudaverdyan, M., Rauschenbeutel, A., and Meschede, D. Precision preparation of strings of trapped neutral atoms. *New J. Phys.* **8**, 191 (2006).

[48] Calarco, T., Dorner, U., Julienne, P. S., Williams, C. J., and Zoller, P. Quantum computations with atoms in optical lattices: Marker qubits and molecular interactions. *Phys. Rev. A* **70**, 012306 (2004).

[49] Zhang, C., Rolston, S. L., and Sarma, S. D. Manipulation of single neutral atoms in optical lattices. *Phys. Rev. A* **74**, 042316 (2006).

[50] Gorshkov, A. V., Jiang, L., Greiner, M., Zoller, P., and Lukin, M. D. Coherent quantum optical control with sub-wavelength resolution. *arXiv:0706.3879v1 [quant-ph]* (2007).

[51] Wei, J. and Norman, E. Lie algebraic solution of linear differential equations. *J. Math. Phys.* **4**, 575 (1963).

[52] Breuer, H.-P. and Petruccione, F. *The theory of open quantum systems*. Oxford University Press, Oxford, (2002).

[53] Doll, R., Zueco, D., Wubs, M., Kohler, S., and Hänggi, P. On the conundrum of deriving exact solutions from approximate master equations. *arXiv:0707.3938v1* (2007).

[54] Ferlaino, F., D'Errico, C., Roati, G., Zaccanti, M., Inguscio, M., Modugno, G., and Simoni, A. Feshbach spectroscopy of a K-Rb atomic mixture. *Phys. Rev. A* **73**, 040702 (2006).

[55] Tiesinga, E., Anderlini, M., and Arimondo, E. Determination of the scattering length of the a $^3\Sigma^+$ potential of $^{87}RbCs$. *Phys. Rev. A* **75**, 022704 (2007).

[56] Anderlini, M., Courtade, E., Cristiani, M., Cossart, D., Ciampini, D., Sias, C., Morsch, O., and Arimondo, E. Sympathetic cooling and collisional properties of a Rb-Cs mixture. *Phys. Rev. A* **71**, 061401(R) (2005).

[57] Dicke, R. H. Coherence in spontanous radiation processes. *Phys. Rev.* **93**, 99 (1954).

[58] Metropolis, N., Rosenbluth, A. W., Rosenbluth, M. N., Teller, A. H., and Teller, E. Equation of state calculations by fast computing mashines. *J. Chem. Phys.* **21**, 1087 (1953).

[59] Binder, K., editor. *Monte Carlo Methods in Statistical Physics*. Springer Verlag, Berlin, second edition, (1986).

[60] Yilmaz, M. B. and Zimmermann, F. M. Exact cluster size distribution in the one-dimensional Ising model. *Phys. Rev. E* **71**, 026127 (2005).

[61] Pleimling, M. and Selke, W. Droplets in the coexistence region of the two-dimensional Ising

model. *J. Phys. A: Math. Gen.* **33**, L199 (2000).

[62] Modugno, G., Modugno, M., Riboli, F., Roati, G., and Inguscio, M. Two atomic species superfluid. *Phys. Rev. Lett.* **89**, 190404 (2002).

[63] Hartmann, T., Keck, F., Korsch, H. J., and Mossmann, S. Dynamics of Bloch oscillations. *New J. Phys.* **6**, 2 (2004).

[64] Ponomarev, A. V., Madroñero, J., Kolovsky, A. R., and Buchleitner, A. Atomic current across an optical lattice. *Phys. Rev. Lett.* **96**, 050404 (2006).

[65] Bruderer, M., Klein, A., Clark, S. R., and Jaksch, D. Transport of strong-coupling polarons in optical lattices. *arXiv:0710.4493v1* (2007).

[66] Schmidt, B., Plimak, L. I., and Fleischhauer, M. Stochastic simulation of a finite-temperature one-dimensional Bose gas: From the Bogoliubov to the Tonks-Girardeau regime. *Phys. Rev. A* **71**, 041601 (2005).

[67] Vidal, G. Efficient simulation of one-dimensional quantum many-body systems. *Phys. Rev. Lett.* **93**, 040502 (2004).

[68] Verstraete, F., García-Ripoll, J. J., and Cirac, J. I. Matrix product density operators: Simulation of finite-temperature and dissipative systems. *Phys. Rev. Lett.* **93**, 207204 (2004).

[69] Clark, S. and Jaksch, D. Dynamics of the superfluid to Mott insulator transition in one dimension. *Phys. Rev. A* **70**, 043612 (2004).

[70] Schulte, T., Drenkelforth, S., Kleine Büning, G., Ertmer, W., Arlt, J., Lewenstein, M., and Santos, L. Dynamics of Bloch oscillations in disordered lattice potentials. *arXiv:0707.3131v1* (2007).

[71] Dankert, C. Efficient simulation of random quantum states and operators. *quant-ph/0512217* (2005).

[72] Pedersen, L. H., Mølmer, K., and Møller, N. M. Fidelity of quantum operations. *quant-ph/0701138* (2007).